Accelerated Gravitational Point Set Alignment with Altered Physical Laws

Vladislav Golyanik[1] Christian Theobalt[1] Didier Stricker[2,3]

1 max planck institut informatik · Graphics Vision & Video · Saarland Informatics Campus SIC
2 Technische Universität Kaiserslautern
3 augmented VISION DFKI

ICCV 2019 Seoul, Korea

CONTRIBUTIONS

- We resolve several limitations of gravitational methods, *i.e., prohibitively high computational complexity, ill-posedness w.r.t the parameters* as well as *a narrow convergence basin for rotation resolution.*
- Moreover, *the number of parameters is reduced, near-field singularities* are *eliminated* and it is shown *how to effectively define boundary conditions with masses.*
- In our formulation, we *preserve the advantages of rigid GA and improve the robustness to uniform noise.* The resulting *Barnes-Hut Rigid Gravitational Approach* (BH-RGA) with altered physical laws outperforms multiple tested baselines.

GRAVITATIONAL METHODS FOR POINT SET ALIGNMENT

$$\mathbf{E}(\mathbf{R},\mathbf{t}) = -G\sum_{i,j}\frac{m_{\mathbf{y}_i}\, m_{\mathbf{x}_j}}{\|\mathbf{R}\,\mathbf{y}_i+\mathbf{t}-\mathbf{x}_j\|_2+\epsilon}$$

$$\vec{\mathbf{f}}_i = -G m_{\mathbf{y}_i}\sum_j m_{\mathbf{x}_j}\left(\|\mathbf{y}_i-\mathbf{x}_j\|^2+\epsilon^2\right)^{-3/2}\hat{\mathbf{n}}_{i,j} - \eta v_i^t$$

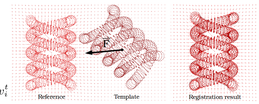

Rigid Gravitational Approach (Second-Order ODEs) [6]

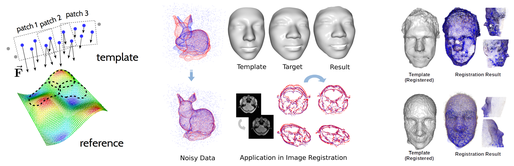

Non-Rigid Gravitational Approach (Second-Order ODEs) [1]

$$F_i^{(ex)} = -\gamma\sum_{j=1}^{M}\frac{m_i m_j}{\|\boldsymbol{q}_i-\boldsymbol{p}_j\|^3}(\boldsymbol{q}_i-\boldsymbol{p}_j)$$

$$F_i^{(ex)} = \kappa\sum_{j=1}^{M}\Delta_i\frac{(\boldsymbol{q}_i-\boldsymbol{p}_j)}{\|\boldsymbol{q}_i-\boldsymbol{p}_j\|^3}$$

$$\Delta_i = 1-\frac{\|\boldsymbol{f}_i^t-\boldsymbol{f}_j^t\|}{\sqrt{D}} \qquad \Delta_i = 2\left(0.5-\frac{\|\boldsymbol{f}_i^t-\boldsymbol{f}_j^t\|}{\sqrt{D}}\right)$$

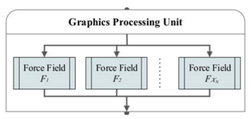

acceleration on a GPU

Feature-Enhanced Physics-Based Approach with Rigid Body Dynamics (Physical Heuristics and Monte-Carlo Simulation) [8]

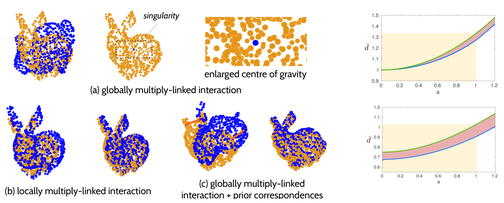

Resolving Scale Singularities [7]

OUR METHOD WITH ALTERED PHYSICAL LAWS

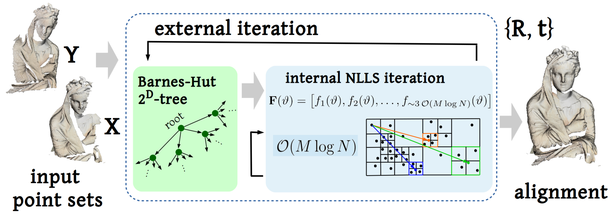

Overview of the proposed BH-RGA approach with accelerated computation of gravitational potential energy (GPE). In contrast to previous approaches relying on second-order ODEs, we apply a *negative elementwise reciprocal transform* to the physically accurate form of GPE and optimise it with non-linear least squares.

Physically-inspired GPE

$$\mathbf{U}(\mathbf{R},\mathbf{t}) = -G\sum_{i,j}\frac{m_{\mathbf{y}_i}\, m_{\mathbf{x}_j}}{\|\mathbf{R}\,\mathbf{y}_i+\mathbf{t}-\mathbf{x}_j\|_2+\epsilon}$$

is minimised by iteratively updating point velocities and displacements [6]:

$$v_i^{t+1} = v_i + \Delta t\,\frac{\vec{\mathbf{f}}_i}{m_{\mathbf{y}_i}} \quad \text{and} \quad d_i^{t+1} = \Delta t\, v_i^{t+1}$$

The proposed transform of GPE:

$$\xi^-\big(\mathbf{U}(\mathbf{R},\mathbf{t})\big) = \sum_{i,j}\frac{1}{G\, m_{\mathbf{y}_i}\, m_{\mathbf{x}_j}}\|\mathbf{R}\,\mathbf{y}_i+\mathbf{t}-\mathbf{x}_j\|_2+\epsilon$$

Our energy after the transform and simplifications:

$$\mathbf{E}(\mathbf{R},\mathbf{t}) = \sum_i\sum_j m_{\mathbf{y}_i}\, m_{\mathbf{x}_j}\,\|\mathbf{R}\,\mathbf{y}_i+\mathbf{t}-\mathbf{x}_j\|_2$$

PROPOSITION. *If located sufficiently far away, the total impact of elements x_k in a volume V to y_i can be approximated by the impact of a single cluster x̃. The mass of x̃ equals to the mass integral of x_k over V, and the position of x̃ equals to the centre of mass of the elements x_k in V [2,6]:*

$$\sum_{k=1}^{K} m_{\mathbf{y}_i}\, m_{\mathbf{x}_k}\,\|\hat{\mathbf{y}}_i-\mathbf{x}_k\|_2 \approx m_{\mathbf{y}_i}\left[\sum_{k=1}^{K} m_{\mathbf{x}_k}\right]\|\hat{\mathbf{y}}_i-\tilde{\mathbf{x}}\|_2$$

GPE WITH BH-TREE. The final GPE of BH-RGA with 2^D -tree acceleration for particle interactions is:

$$\mathbf{E}(\mathbf{R},\mathbf{t}) = \sum_{\forall \mathbf{y}_i}\; \sum_{\mathbf{k}_j\in\mathcal{K}(\mathbf{y}_i)} m_{\mathbf{k}_j}\,\|\mathbf{R}\,\mathbf{y}_i+\mathbf{t}-\mathbf{k}_j\|_2$$

where $\mathbf{k}_j \in \mathcal{K}(\mathbf{y}_i)$ denotes fetchable representations of the reference point set.

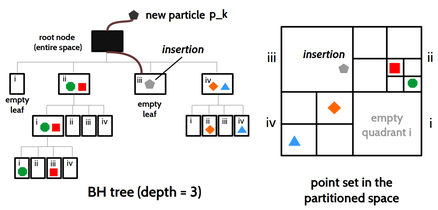

Insertion rule for building a 2^D -tree, the case of an empty external node.

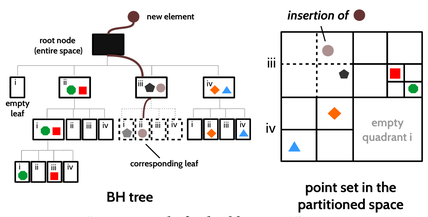

Insertion rule for building a 2^D-tree, the case of non-empty internal or external node.

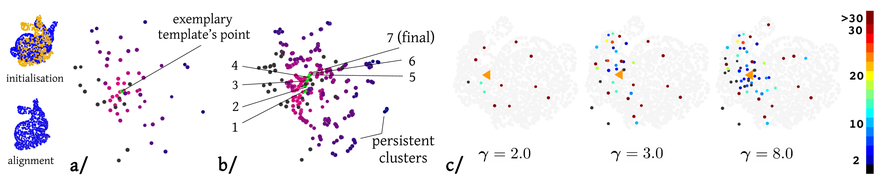

Visualisation of clusters in BH-RGA: a/ cluster configuration in the beginning; b/ overlayed configurations for all seven iterations; c/ cluster configuration in the first iteration, for a single template point (shown as a triangle) and three different γ values.

EXPERIMENTS

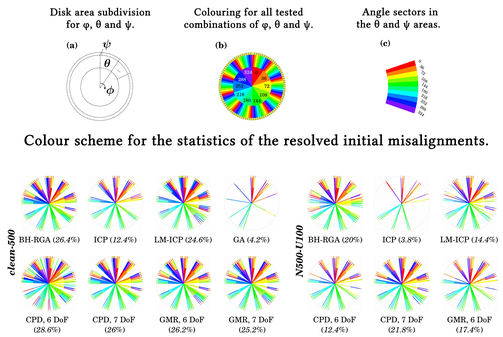

Colour-coded statistics of the resolved initial misalignments in the clean-500 and N500-U100 experiments.

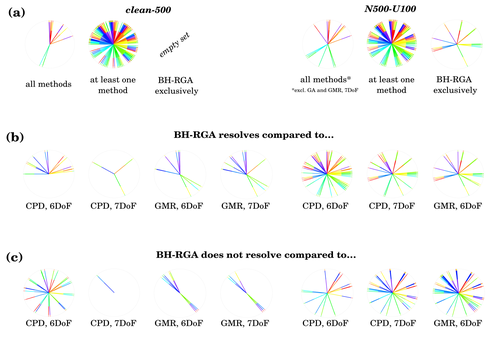

Colour-coded comparative statistics of the resolved initial misalignments in the clean-500 and N500-U100 experiments. (a): Joint statistics for all methods. (b), (c): Statistics for BH-RGA *vs.* CPD [10] and GMR [9].

methods and metrics		*clean-500*	*N500-U50*	*N500-U100*	*N500-U100*	*U100*	*G100*	*GS100*
ICP [3]	success (in %)	62 (12.4%)	36 (7.2%)	19 (3.8%)	19 (3.8%)	33 (66%)	**50 (100%)**	**50 (100%)**
	RMSE (σ)	0.005 (0.016)	0.022 (0.3)	0.042 (0.031)	0.042 (0.031)	0.091 (0.081)	**0.007 (0.002)**	**0.002 (5.E-4)**
LM-ICP [5]	success (in %)	123 (24.6%)	82 (16.4%)	72 (14.4%)	72 (14.4%)	49 (98%)	**50 (100%)**	**50 (100%)**
	RMSE (σ)	0.002 (6.3E-4)	0.015 (0.009)	0.023 (0.017)	0.023 (0.017)	0.025 (0.021)	**0.006 (0.003)**	**0.003 (0.001)**
CPD (7 DoF) [10]	success (in %)	130 (26%)	**128 (25.6%)**	**109 (21.8%)**	**109 (21.8%)**	48 (96%)	**50 (100%)**	**50 (100%)**
	RMSE (σ)	0.04 (6.E-5)	**0.064 (0.003)**	**0.088 (0.003)**	**0.088 (0.003)**	0.098 (0.066)	**0.027 (1.7E-3)**	**0.046 (1.7E-3)**
CPD (6 DoF) [10]	success (in %)	**143 (28.6%)**	98 (19.6%)	62 (12.4%)	62 (12.4%)	48 (96%)	**50 (100%)**	**50 (100%)**
	RMSE (σ)	**0.006 (0.009)**	0.023 (0.014)	0.034 (0.017)	0.034 (0.017)	0.061 (0.148)	**0.01 (0.003)**	**7.5E-3 (2.3E-3)**
GMR (7 DoF) [9]	success (in %)	126 (25.2%)	113 (22.6%)	0 (0%)	0 (0%)	0 (0%)	**50 (100%)**	**50 (100%)**
	RMSE (σ)	7.E-5 (8.E-5)	0.084 (0.005)	n / a	n / a	n / a	**0.04 (7.5E-3)**	**1.5E-3 (4.7E-4)**
GMR (6 DoF) [9]	success (in %)	131 (26.2%)	79 (15.8%)	87 (17.4%)	87 (17.4%)	36 (72%)	26 (52%)	25 (25%)
	RMSE (σ)	8.E-5 (2.E-4)	5.E-4 (2.E-4)	6.E-4 (2.E-4)	6.E-4 (2.E-4)	0.16 (0.077)	0.37 (0.4)	0.37 (0.38)
GA [6]	success (in %)	21 (4.2%)	6 (1.2%)	3 (0.6%)	3 (0.6%)	19 (38%)	1 (2%)	10 (20%)
	RMSE (σ)	0.029 (0.021)	0.049 (0.025)	0.03 (0.012)	0.03 (0.012)	0.164 (0.082)	0.289 (0.087)	0.163 (0.072)
BH-RGA (ours)	success (in %)	132 (26.4%)	**132 (26.4%)**	**100 (20%)**	**100 (20%)**	**50 (100%)**	**50 (100%)**	**50 (100%)**
	RMSE (σ)	0.009 (0.004)	**0.032 (0.013)**	**0.059 (0.021)**	**0.059 (0.021)**	**0.056 (0.017)**	**0.04 (0.01)**	**0.022 (0.006)**

Quantitative evaluation on clean-500, N500-U50, N500-U100, U100, G100 and GS100.

$$\rho(\mathcal{D}_t) = \mathbf{F}_{3\times M} = [\mathbf{f}_i] = (\mathbf{R}-\mathbf{I})\mathbf{Y}+\mathbf{T} \qquad \text{3D scene flow}$$

$$\rho_{2D}\colon \Omega\subset\mathbb{R}^2 \to \mathbb{R}^2 \qquad \text{2D projection of scene flow}$$

$$\pi_\rho\colon \mathbb{Z}^2\times\mathbb{R}\times\mathbb{R}^3 \to \mathbb{R}^2$$

$$\pi_\rho(x,y,\mathbf{P}_z,\mathbf{f}_i) = \begin{bmatrix} f_x\,\frac{\mathbf{f}_{i,x}+\mathbf{P}_x}{\mathbf{f}_{i,z}+\mathbf{P}_z}+(c_x-x) \\ f_y\,\frac{\mathbf{f}_{i,y}+\mathbf{P}_y}{\mathbf{f}_{i,z}+\mathbf{P}_z}+(c_y-y)\end{bmatrix} \qquad \text{scene flow projection operator}$$

$$\mathbf{P} = \pi^{-1}(x,y,\mathbf{P}_z),\ \mathbf{P}_z = \mathcal{D}_t(x,y)$$

$$\pi^{-1}(x,y,z) = \left(z\frac{(x-c_x)}{f_x}, z\frac{(y-c_y)}{f_y}, z\right) \qquad \text{inverse projection operator}$$

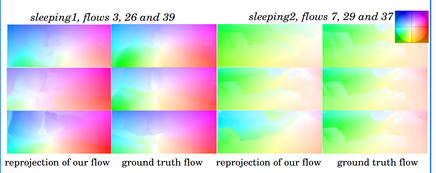

Examples of reprojected 3D displacements obtained by BH-RGA, compared to ground truth optical flows from SINTEL [4].

evaluated configuration		*RMSE*	*σ*	*cases (success rate)*
E-CPD [10]* prior matches only	[no priors]	0.08	0.013	85 (17%)
	1 prior	0.084	0.012	89 (18%)
	2 priors	0.076	0.014	376 (75%)
	3 priors	0.056	0.018	488 (97%)
BH-RGA (ours), *anchor points*	[no priors]	**0.05**	**0.018**	**124 (25%)**
	1 prior	**0.043**	**0.013**	**199 (40%)**
	2 priors	**0.011**	**0.017**	191 (38%)
	3 priors	**0.0086**	**0.005**	165 (33%)
BH-RGA (ours), *prior matches*	1 prior	**0.0191**	**1.1E-4**	**435 (87%)**
	2 priors	**0.0055**	**1.72E-5**	**500 (100%)**
	3 priors	**0.0001**	**4.5E-9**	**500 (100%)**

RMSE and std. dev. for *U256* and *G256*.

method	*U256*	*G256*
ICP [3]	**9.E-3 (7.E-3)**	**0.015 (0.012)**
LM-ICP [5]	0.077 (0.041)	0.113 (0.063)
CPD (7 DoF) [10]	0.051 (9.E-3)	0.064 (0.021)
CPD (6 DoF) [10]	0.016 (0.014)	0.045 (0.058)
GMR (7 DoF) [9]	0.019 (0.028)	0.065 (0.051)
GMR (6 DoF) [9]	0.853 (1.16)	1.027 (1.226)
GA [6]	0.149 (0.143)	0.207 (0.158)
BH-RGA (ours)	**0.015 (4.E-3)**	**0.019 (9.5E-3)**

Comparison of E-CPD and BH-RGA (ours).

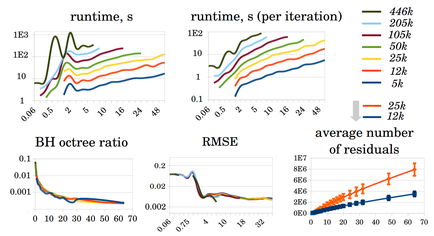

Runtime evaluation metrics as the functions of γ (SINTEL *sleeping2* [4], different sub-sampling rates and number of points).

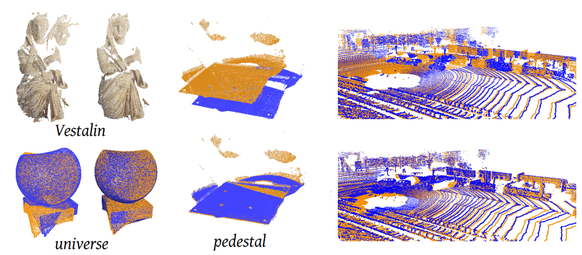

Exemplary alignments of real-world data with BH-RGA.

ALGORITHM PARAMETERS AND THE LOWER BOUND ON GPE

parameter	*interpretation*
G	gravitational constant
$m^{\mathbf{X}_j}$	default mass of template points
$m^{\mathbf{Y}_i}$	default mass of reference points
ε	softening length
η	strength of energy dissipation
Δt	forward integration step
$\vec{v}_{\mathbf{Y}}^{\,0}$	*initial template's velocity (optional)*

Parameters of GA [6]

parameter	*interpretation*
ϵ	Huber loss threshold
γ	distance threshold of 2^D-tree
$m_{\mathbf{y}_i}$	*template point masses (optional)*
$m_{\mathbf{x}_j}$	*reference point masses (optional)*

Parameters of BH-RGA (ours)

$$\lim_{\|\mathbf{R}\mathbf{Y}+\mathbf{T}\|_{\mathcal{F}}\to\|\mathbf{X}\|_{\mathcal{F}}} \mathbf{U}(\mathbf{R},\mathbf{t}) = -\infty, \qquad \lim_{\|\mathbf{R}\mathbf{Y}+\mathbf{T}\|_{\mathcal{F}}\to\|\mathbf{X}\|_{\mathcal{F}}} \xi^-\big(\mathbf{U}(\mathbf{R},\mathbf{t})\big) = 0.$$

The further two particles are apart from each other, the higher is the GPE between them.

PRIOR MATCHES AND ANCHOR POINTS

$$\mathbf{E}^p(\mathbf{R},\mathbf{t}) = \begin{cases}\mathbf{E}(\mathbf{R},\mathbf{t}) & \forall \mathbf{y}_i : i\notin N_c, \quad \text{for all points without a prior match}\\ m^p_{\mathbf{y}_i} m^p_{\mathbf{x}_j}\,\|\mathbf{R}\,\mathbf{y}_i+\mathbf{t}-\mathbf{x}_j\|_2, & \text{else} \quad \text{for all prior matches}\end{cases}$$

Increasing the masses $m^p_{\mathbf{y}_i} m^p_{\mathbf{x}_j}$ in GPE leads to anchor points (weak prior correspondences).

REFERENCES

1. S. A. Ali *et al.* NRGA: Gravitational Approach for Non-Rigid Point Set Registration. In *3DV*, 2018.
2. J. Barnes and P. Hut. A hierarchical o(n log n) force-calculation algorithm. *Nature*, 1986.
3. P. J. Besl and N. D. McKay. A method for registration of 3-d shapes. *TPAMI*, 1992.
4. D. J. Butler *et al.* A naturalistic open source movie for optical flow evaluation. In *ECCV*, 2012.
5. A. W. Fitzgibbon. Robust registration of 2D and 3D point sets. In *BMVC*, 2001.
6. V. Golyanik *et al.* Gravitational Approach for Point Set Registration. In *CVPR*, 2016.
7. V. Golyanik and C. Theobalt. Optimising for Scale in Globally Multiply-Linked Gravitational Point Set Registration Leads to Singularities. In *3DV*, 2019.
8. P. Jauer *et al.* Efficient Registration of High-Resolution Feature Enhanced Point Clouds. *TPAMI*, 2019.
9. B. Jian and B. C. Vemuri. Robust point set registration using gaussian mixture models. *TPAMI*, 2011.
10. A. Myronenko and X. Song. Point Set Registration: Coherent Point Drift. *TPAMI*, 2010.